

Revision of the nautical bottom concept in the harbour of Zeebrugge through ship model testing and manoeuvring simulation

Guillaume Defoortrie, Marc Vantorre

Division of Maritime Technology, Ghent University (Belgium)

Katrien Eloot, Erik Laforce

Flanders Hydraulics Research, Antwerp (Belgium)

1. INTRODUCTION

Many navigational channels have bottoms that are covered with fluid mud suspensions, characterised by low density ($1050\text{--}1300\text{ kg/m}^3$) and weak shear strength. In such conditions, the bottom level is not clearly defined, as traditional survey techniques appear to be inadequate. In muddy areas it is therefore appropriate to introduce the *nautical bottom* concept, defined as *the level where physical characteristics of the bottom reach a critical limit beyond which contact with a ship's keel causes either damage or unacceptable effects on controllability and manoeuvrability* (PIANC, 1997). In case of bottoms covered with fluid mud layers, this nautical bottom is located at some depth under the water-mud interface where, from rheological point of view, a transition between fluid and solid mud can be defined. In harbours where the nautical bottom concept is applied, the operational definition of this level is usually linked to a critical density value, varying between 1150 and 1270 kg/m^3 .

The choice of a critical density is based on considerations about the rheological properties of the local mud. In the harbour of Zeebrugge, a critical value of 1150 kg/m^3 has been selected based on a large number of simultaneous point measurements of both rheology and density profiles. As the rheological transition level was always located below the 1150 kg/m^3 horizon, the latter is nowadays considered to be the nautical bottom and is displayed on the nautical charts in areas where high and low frequency echo soundings yield different results.

The introduction in the 1980s of the nautical bottom concept in the access channels to the harbour of Zeebrugge has resulted into a significant reduction of the maintenance dredging cost. More recent rheological in situ measurements, however, have revealed that the mud characteristics, and in particular the depth – rheology relationship, have changed significantly. Two rheological transition levels can be defined: a first transition, at which the rheological characteristics increase slightly, occurs at a density between 1.08 and 1.12 ton/m^3 ; a more severe transition takes place in a density range from 1.18 to 1.25 kg/m^3 (see figure 1.1).

Based on these results, suggestions were made to increase the critical density level from 1.15 to higher values, so that a larger part of the fluid mud layer could be incorporated into the under keel clearance. As at several locations this would cause contact between the ship's keel and the mud layer, the effect of such a decision on a ship's behaviour and, as a result, on safety of shipping traffic, had to be investigated

thoroughly. For this reason, a comprehensive research program was carried out at Flanders Hydraulics Research (Antwerp, Belgium) with the scientific support of Ghent University.

The present paper gives an overview of the followed approach, involving model tests, fast time simulation runs and real time simulations at a full mission bridge simulator, as well as a presentation of the preliminary conclusions.

2. EXPERIMENTAL PROGRAM

2.1 Test facilities

Flanders Hydraulics, the hydraulic research station of the Waterways and Maritime Affairs Administration of the Ministry of Flanders, is particularly concerned with investigation of ship hydrodynamics for problems in relation with the concept, adaptation and operation of navigation areas. Therefore, the (very) shallow water range is a main research domain.

For the investigation of nautical aspects of these problems, a ship manoeuvring simulator has been installed. In order to provide the mathematical model of this simulator with realistic data, the availability of experimental facilities was considered as a requirement. At present these facilities consist of a shallow water towing tank ($88\text{ m} \times 7.0\text{ m} \times 0.6\text{ m}$), equipped with a planar motion carriage, a wave generator and an auxiliary carriage for ship-ship interaction tests. Thanks to computerised control and data-acquisition, the facilities are operated in a fully automatic mode.

2.2 Ship models

Two $1/75$ -scale models, a container carrier (model "D": $L_{pp} = 289.8\text{ m}$; $B = 40.25\text{ m}$; $T = 13.50\text{ m}$; $C_B = 0.59$); and a tanker, the *Esso Osaka* (model "E": $L_{pp} = 286.8\text{ m}$; $B = 46.77\text{ m}$; $T = 15.50\text{ m}$; $C_B = 0.82$) were selected. Most experiments have been carried out with the container carrier. Both ship models were equipped with a propeller and a rudder.

2.3 Bottom conditions

The mud was simulated by a mixture of two types of chlorinated paraffin and petrol, so that both density and viscosity could be controlled within certain ranges. For environmental reasons, the tank was divided into three compartments: a test section, a "mud"

reservoir and a water reservoir. Bottom and walls were covered with a polyethylene coating.

The selected density-viscosity combinations and the tested bottom conditions are represented in Table 1. This selection was based on measurements of density and rheology profiles in situ carried out in the outer harbour of Zeebrugge in 1997-98. A mud layer configuration is defined by two characters: a letter ("b", ..., "h"), denoting the material characteristics and a figure ("1", "2", "3"), representing the layer thickness. Tests carried out above a solid bottom are referred to as "S".

For ship model "D" the gross under keel clearance of the ship relative to the tank bottom was varied between 7 and 32% of draft, yielding an under keel clearance relative to the mud-water interface varying between -12 and +21%. For model "E" the values for the under keel clearance were extended between 10 and 15% of draft referred to the tank bottom, and from -10% to +10% relative to the mud-water interface.

Table 1. Bottom conditions and tested models.

Mud type	Density (kg/m ³)	Dynamic viscosity (Pa s)	Layer thickness		
			0.75 m "1"	1.50 m "2"	3.00 m "3"
"d"	1100	0.03	D/E	D/E	D/E
"c"	1150	0.06	D	D	D
"b"	1180	0.10	D	D	D
"f"	1200	0.11	-	D	-
"h"	1210	0.19	D/E	D/E	D
"e"	1260	0.29	-	D	-
"g"	1250	0.46	-	D/E	D/E
"S"	solid bottom				

2.4 Test types

For each combination of mud type, layer thickness and under keel clearance, a captive test program was carried out for determining mathematical manoeuvring models covering a range of forward speeds between 2 knots astern and 10 knots ahead.

The experimental program consisted of: bollard pull tests with varying rudder angle and propeller rate; stationary tests with varying forward speed, rudder angle, drift angle and propeller rpm; harmonic sway and yaw tests; multimodal tests with variable speed, rudder angle and/or propeller rpm.

During the captive manoeuvring tests, following data were measured: longitudinal force components fore and aft, lateral force component fore and aft, vertical motion at four measuring posts (fore/aft, port/starboard), normal and tangential rudder force components, rudder torque, rudder angle, propeller torque, thrust and rpm. In particular cases, the vertical motion of the mud-water and water-air interfaces was registered as well.

3 MATHEMATICAL MANOEUVRING MODEL

3.1 General concept

Based on the results of the captive model tests, a mathematical manoeuvring model for simulation purposes has been developed for each combination of bottom condition and under keel clearance. The mathematical models are of the modular type, so that the force and moment components are expressed as a sum of hydrodynamic reactions on the hull, and terms induced by the propeller and rudder action:

$$F = F_H + F_P + F_R \quad (1)$$

As the mathematical models have to be valid in a broad range of conditions (four-quadrant propeller action, 360 deg drift and yaw angle), it was decided to formulate force components by determining functions of non-dimensional parameters in a tabular form, rather than attempting to define analytical expressions.

3.2 Hull forces

Following formulation of X (longitudinal force component), Y (lateral force component) and N (yawing moment) acting on the hull due to hydrodynamic action and inertia was found to be adequate for all bottom configurations and under keel clearances:

$$X_H = \left(X_u(u) - m \right) \dot{u} + m v r + m x_G r^2 + \left[X_{vv}(u) \dot{v}^2 + X_{vv}(u) \dot{v} + X_{rr}(u) \dot{r}^2 + X_{rr}(u) \dot{r} \right] + \frac{1}{2} \rho L T \left\{ \left(u^2 + v^2 \right) X'(\beta) + \left(u^2 + \left(\frac{rL}{2} \right)^2 \right) X'(\gamma) + \left(v^2 + \left(\frac{rL}{2} \right)^2 \right) X'(\chi) \right\} \quad (2)$$

$$Y_H = \left(Y_v - m \right) \dot{v} + \left(Y_r(\beta) - m x_G \right) \dot{r} - m u r + \frac{1}{2} \rho L T \left\{ \left(u^2 + v^2 \right) Y'(\beta) + \left(u^2 + \left(\frac{rL}{2} \right)^2 \right) Y'(\gamma) + \left(v^2 + \left(\frac{rL}{2} \right)^2 \right) Y'(\chi) \right\} \quad (3)$$

$$N_H = \left(N_v - m x_G \right) \dot{v} + \left(N_r (\beta) - I_{zz} \right) \dot{r} - m x_G u r + \frac{1}{2} \rho L^2 T \left\{ \begin{aligned} & \left(u^2 + v^2 \right) N'(\beta) + \left(u^2 + \left(\frac{rL}{2} \right)^2 \right) N'(\gamma) \\ & + \left(v^2 + \left(\frac{rL}{2} \right)^2 \right) N'(\chi) \end{aligned} \right\} \quad (4)$$

u , v , r being the longitudinal and lateral velocity components and the yaw rate, respectively; m denotes the ship's mass, I_{zz} the inertia moment about the vertical z -axis, and x_G the longitudinal position of the centre of gravity.

All functions of $\beta = \arctan\left(-\frac{v}{u}\right)$, $\gamma = \arctan\left(\frac{rL}{2u}\right)$, $\chi = \arctan\left(\frac{rL}{2v}\right)$, u are expressed in tabular form.

Following results are of interest for a better insight into the physical mechanisms determining a ship's behaviour in muddy navigation areas:

- The non-dimensional resistance of the ship is shown as a function of under keel clearance for several bottom conditions in Figure 3.1. Contact with high density mud layers leads to a dramatic, very sharp increase of resistance, while the interface does not appear to be a strict boundary in case of lower density mud.
- Hydrodynamic inertia ("added mass") terms for sway and yaw increase significantly with decreasing water depth and increasing density and viscosity of the mud layer, as is illustrated in Figure 3.2. In case the ship's keel penetrates deep into the mud, very large values are observed, up till seven times the ship's mass. The layer characteristics appear to be important parameters, even if no contact occurs with the mud layer: the shallow water effect is smoothened with increasing layer thickness and decreasing mud density and viscosity. Indeed, an abrupt transition cannot be observed at $h_1/T = 1$.
- The magnitude of lateral force and yawing moment due to drift increases significantly with decreasing water depth. This is illustrated in Figure 3.3a, displaying the non-dimensional lateral force due to drift for several bottom conditions. However, this increase appears to stagnate when the keel touches the interface; penetration into the mud layer does not result into a further increase. For a given positive under keel clearance relative to the interface, the presence of a mud layer appears to smoothen the shallow water effects, especially in case of low density and viscosity layers (Figure 3.3b). The effect of mud properties on the lateral force acting on a ship in contact with mud is displayed in figure 3.3c.
- The evolution of the yaw induced lateral force and yawing moment is of particular interest. Similar to $Y(\beta)$, the magnitude of the yaw damping moment

$N(\gamma)$ gradually increases with decreasing under keel clearance and stagnates once the ship's keel touches the mud layer. The hydrodynamic lateral force due to yaw, which is practically negligible in deep water compared with the centrifugal force ($-mur$), appears to be of increasing importance and counteracts the centrifugal inertia force completely at extremely small positive under keel clearances in this specific case, as shown in Figure 3.4, making use of the linearised approach (Y_{wru}). For smaller and negative under keel clearances, the resulting lateral force due to yaw is even centripetal. The transition from centrifugal to centripetal action takes place at larger values of the under keel clearance when the density and viscosity of the mud layer increase and the thickness of the layer decreases. Therefore, this effect is not to be considered as a typical characteristic for ship behaviour in muddy areas, but rather as a (very) shallow water effect.

3.3 Propeller induced forces

The longitudinal force acting on the ship due to propeller action is given by:

$$X_P = (1-t)T_P \quad (5)$$

t being the thrust deduction factor, and T_P the propeller thrust. A larger value for t – which implies a smaller longitudinal force for a given thrust – is obtained at positive under keel clearances relative to the interface with high density mud layers; if the ship's keel touches the mud, on the other hand, t is larger for the lightest mud layers.

The propeller thrust can be expressed as follows:

$$T_P = \frac{(0.7)^2}{8} \pi^3 \rho n^2 D_P^4 C_T(\epsilon) (1 + \tan^2 \epsilon) \quad (6)$$

D_P being the propeller diameter, n the propeller rate (rps), and $C_T(\epsilon)$ being the open water thrust characteristic:

$$C_T(\epsilon) = \frac{T_P}{\frac{1}{2} \rho A_0 [u^2 + (0.7\pi n D_P)^2]} \quad (7)$$

expressed as a function of the advance angle ϵ :

$$\epsilon = \text{Arctan}\left(\frac{u_P}{0.7\pi n D_P}\right) = \text{Arctan}\left(\frac{u(1-w)}{0.7\pi n D_P}\right) \quad (8)$$

which requires an expression of the wake factor w . The latter can be expressed as a function of the appar-

ent advance angle $\varepsilon^* = \text{Arctan}\left(\frac{u}{0.7\pi nD_P}\right)$, and appears to be influenced significantly by the bottom condition (see figure 3.5):

- the wake factor increases with decreasing mud density, which implies an obstruction of the flow to the propeller; this phenomenon can be ascribed to the vertical interface motions;
- contact between the ship's keel and higher density mud layers causes an inflow of two fluids into the propeller, resulting into higher thrust and torque and, therefore, small wake factor values.

Figure 3.6 shows that the effect of the presence of mud on the overall efficiency of the propeller: compared to a solid bottom, a significant loss of efficiency is stated, especially for negative under keel clearances.

Besides a longitudinal force, propeller action also causes a lateral force and a yawing moment, due to asymmetry of the flow. This phenomenon is especially important in the 2nd and 4th quadrant (combination of forward speed and backing propeller, or motion astern and propeller ahead). In shallow water, it is observed that these actions are not constant in time, but contain an important slowly oscillating component, the amplitude of which is in the order of magnitude of the propeller thrust. This effect was also included in the mathematical model (see figure 3.7).

3.4 Rudder induced forces

For the forces acting on the rudder, the following formulation is adapted:

$$\begin{aligned} F_X &= \frac{\rho}{2} A_R V_R^2 [C_L(\alpha_R) \sin\beta_R + C_D(\alpha_R) \cos\beta_R] \\ F_Y &= \frac{\rho}{2} A_R V_R^2 [C_L(\alpha_R) \cos\beta_R - C_D(\alpha_R) \sin\beta_R] \end{aligned} \quad (9)$$

A_R being the lateral rudder surface and C_L and C_D the lift and drag coefficients in open water, respectively. The inflow angle $\alpha_R = \delta_R + \delta_0 + \beta_R$ is determined by the rudder angle δ_R , an offset angle δ_0 and the local drift angle $\beta_R = \arctan(-v_R/u_R)$ at the rudder ($x=x_R$). The local longitudinal and lateral flow components also determine the inflow velocity $V_R = (u_R^2 + v_R^2)^{1/2}$; they are expressed as follows:

$$u_R = \frac{1 - w_{R0}}{1 - w_P} \cdot \sqrt{\eta \left[(1 - k) \sin\varepsilon + k \sqrt{(C_T + \sin^2\varepsilon)} \right]^2 + (1 - \eta) \sin^2\varepsilon} \cdot \left[\left((1 - w_P) u \right)^2 + (0.7\pi nD_P)^2 \right]^{1/2} \quad (10)$$

$$v_R \approx (v + r x_R) \quad (11)$$

w_{R0} is the wake factor at the rudder; different values are considered for the longitudinal and lateral rudder force components F_X and F_Y . The wake factors depend on the rudder angle δ_R : the largest values are obtained at low δ_R . The bottom condition and the under keel clearance appear to have a significant influence on the $w_{R0,X}$ and $w_{R0,Y}$: the wake factors decrease – and, consequently, the flow to the rudder improves – with increasing mud density and with increasing under keel clearance (figure 3.8). As a result, the inflow to the rudder is very unfavourable when the ship penetrates deep into soft, low density mud layers.

A rudder deviation not only causes a force on the rudder, but asymmetric flow inducing a force $a_H F_Y$ on the hull, with point of application x_H . The factor a_H increases with decreasing under keel clearance and with decreasing mud layer thickness. The application point is always located aft, but rather close to midships; it is moving forward with decreasing under keel clearance and decreasing mud layer thickness. Compared to a solid bottom situation, the application point is located more aft for positive under keel clearances, especially for low density mud layers.

4 REAL-TIME SIMULATION RUNS

4.1 Purpose

The final purpose of the research program consisted in determining operational limits for the navigation in muddy areas, more specifically in the harbour of Zeebrugge. As the pilots play a central role in the navigation to and from Zeebrugge, the input of their experience and assessment in this project was required. For a selection of bottom conditions, a real-time simulation programme was organised with Zeebrugge pilots at the full mission bridge simulator of Flanders Hydraulics Research, Antwerp. All runs were carried out with a container carrier (length over all: 300.0 m; beam: 40.25 m; draft: 13.5 m) calling at and departing from the harbour of Zeebrugge.

The simulation programme was composed paying attention to several aspects:

- Validation of the mathematical models: is the behaviour of the ship assessed as realistic during the simulation runs? In order to evaluate this aspect, simulations were carried out above a solid bottom and above muddy bottoms with reduced under keel clearance, according to existing or realistic situations.
- Determination of the limits of the controllability: according to the PIANC definition, contact between the nautical bottom and the ship's keel causes unacceptable effects on controllability and manoeuvrability. In order to make an assessment in these matters, a series of simulation runs was carried out during which contact occurred between the ship's keel and mud layers with higher density and viscosity.

- Evaluation of the navigability of mud layers: in case it is decided to determine the nautical bottom by means of a density level higher than the present 1.15 t/m^3 , the ship's keel will possibly penetrate into mud layers with reduced density and viscosity. The ship's behaviour in such conditions was assessed by a series of simulation runs.

4.2 Simulation programme

In total, 63 runs were carried out by 15 pilots during 8 days.

A selection of four manoeuvres was considered (see Figure 4.1):

- (1) Arrival, berthing on starboard side at quay 205;
- (2) Arrival, berthing on port side at quay 205;
- (3) Departure from quay 205, moored on port side;
- (4) Arrival at Flanders Container Terminal.

These manoeuvres are typical for large container carriers calling at Zeebrugge, so that a feedback to the pilots' experience was guaranteed; moreover, a broad range of hydrodynamic conditions (speeds ahead/astern, propeller rpm ahead/astern, drift angles, yaw rates, ...) was covered during the simulation runs.

During each single run, the bottom characteristics were assumed to be constant over the entire harbour area. The selected bottom conditions are displayed in figure 4.2.

The access channel to the harbour, the *Pas van het Zand*, is characterised by important tidal currents in the zone beyond the breakwaters; at low tide, the magnitude of cross currents takes values of 2 to 2.5 knots. As these currents greatly affect the shipping traffic arriving and departing from Zeebrugge, realistic current patterns were introduced into the simulation environment.

All manoeuvres were carried out in frequently occurring, moderate wind conditions (SW, 4 Bf); during some runs, more severe winds were applied.

Tug assistance was guaranteed by two tugs of 45 ton bollard pull each; during some runs the available tug power was increased.

4.3 Qualitative evaluation of the simulation runs

All pilots were requested to complete a questionnaire just after the simulation run; this resulted into a first, very important assessment of the manoeuvres. According to the opinion of a large majority of the pilots, the simulation of the outside view, the ship's behaviour and the tug assistance could be considered as "good" to "very good".

After each run, the pilot was asked whether it would be advisable to carry out the manoeuvre in reality. Based on this assessment, the conditions were classi-

fied as "acceptable", "marginal" and "unacceptable"; the results are shown in Figure 4.2.

4.4 Analysis based evaluation of the simulation runs

Taking account of the comments of the pilots on the simulated manoeuvres, it was clear that three criteria should be considered for assessing the bottom conditions:

- Speed: is a departing ship (trajectory 3, sub-trajectory 4) able to reach a speed that is sufficient to compensate for the cross current acting beyond the breakwaters?
- Controllability by own means: can a departing ship (trajectory 3, sub-trajectory 4) obtain a straight course without extreme use of rudder and propeller?
- Manoeuvrability with tug assistance: are the ship's control devices (rudder, propeller) and the tug assistance sufficient to perform the manoeuvres safely within acceptable time limits?

Based on the pilots' qualitative assessment, limits were determined to quantify these criteria:

- Speed: in order to keep within the fairway, a departing ship's speed should be at least 8 knots, and preferably 10 knots. These values were selected as limits for unacceptable, marginal and acceptable conditions.
- For a departing ship's controllability by own control devices, the standard deviation of the rate of turn during sub-trajectory 4 appears to be an adequate indicator. For the different bottom conditions, this value is displayed as a function of the water depth to draft ratio. Taking account of the pilots' evaluation, values of 5 and 6 deg/min were selected as critical limits.
- In order to evaluate the ship's manoeuvrability with tug assistance in a quantitative way, the *impulse of steering force* was introduced, being the time integral of the sum of the lateral rudder and tug induced forces. Similarly, the *impulse of steering moment* was defined as well. The values of these impulses were calculated for each sub-trajectory, and compared to the pilots' evaluation of the adequacy of tug assistance. In this way, it was not only possible to quantify the third criterion, but extrapolations to assistance by more or less powerful tugs could be made as well.

5 CONCLUSIONS

As a result of the analysis of the real-time simulation runs with a small negative under keel clearance, it can be concluded that contact with mud layers of a density of 1.20 t/m^3 or more should be avoided, even if sufficient tug assistance is available. Taking account of the PIANC definition, this value can be considered as a new criterion for the determination of the nautical bottom in the Zeebrugge harbour area.

However, the pilots should always be aware of the level of the water-mud interface, which should be indicated on the nautical charts as well, for several reasons:

- If the ship's keel penetrates by more than 10% of her draft into low density mud layers, this may result into unacceptable situations.
- Small positive under keel clearances relative to the mud-water interface may result into a modification of the ship's behaviour and controllability.

An major conclusion of the simulation study concerns the importance of available tug assistance. If insufficient tug power is available, contact with the mud layer should be avoided, so that the nautical bottom is moved to the mud-water interface; if more powerful tugs can assist the ship, the pilot may decide to allow a larger negative under keel clearance.

In the near future, the tracks, controls and tug assistance of deep-drafted containers ships arriving at and departing from Zeebrugge at low tide will be recorded by the pilots in order to provide a feedback to the simulation study. After an evaluation phase, it will be decided whether the new criteria for the determination of the nautical bottom will be applied in practice.

6 ACKNOWLEDGEMENTS

The research project *Determination of the nautical bottom in the harbour of Zeebrugge: Nautical implications* was carried out co-operatively by Ghent University and Flanders Hydraulics Research (Antwerp), commissioned by T.V. Noordzee & Kust (Ostend) – a joint venture of NV Baggerwerken Decloedt & Zoon, NV Dredging International and NV Ondernemingen Jan De Nul – in the frame of the optimisation of the maintenance dredging contract for the harbour of Zeebrugge, financed by the Department Maritime Access of the Ministry of Flanders, Waterways and Maritime Affairs Administration. The real-time simulation programme was carried out in close co-operation with the Flemish Pilotage.

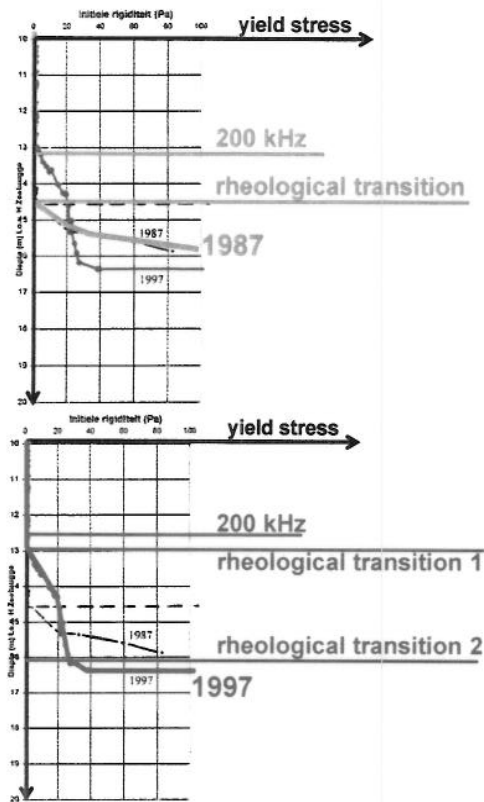


Figure 1.1: Rheology as a function of depth in Zeebrugge harbour, according to measurements in 1987 and 1997.

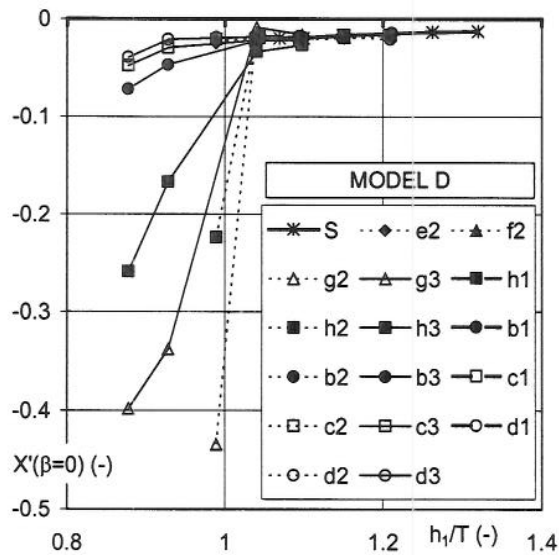


Figure 3.1: Ship model D. Ship resistance: influence of bottom characteristics and under keel clearance.

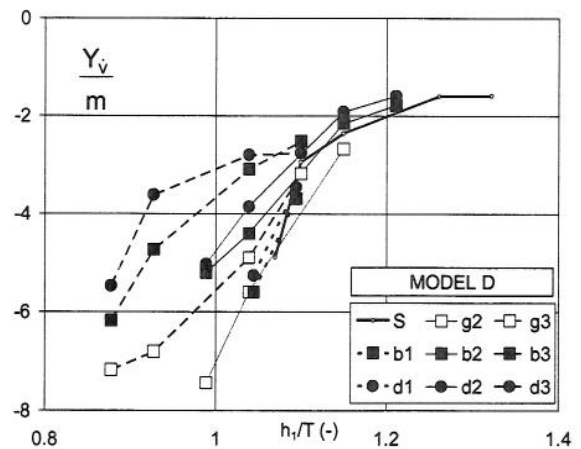


Figure 3.2: Ship model D. Sway added mass: influence of bottom characteristics and under keel clearance.

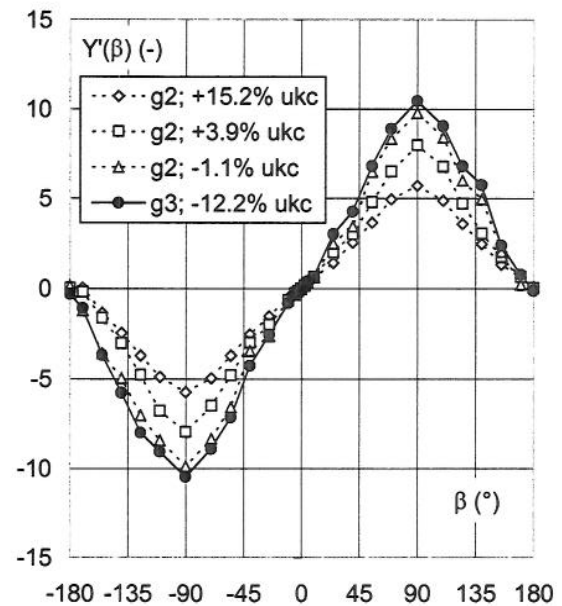


Figure 3.3a: Ship model D. Drift induced lateral force: influence of under keel clearance.

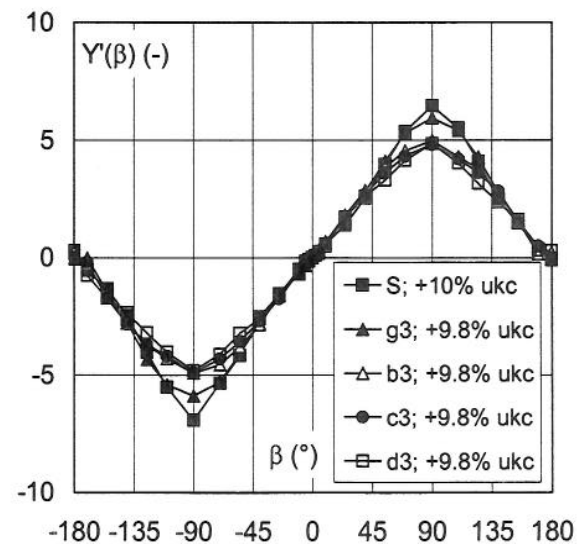


Figure 3.3b: Ship model D. Drift induced lateral force: influence of bottom characteristics for positive under keel clearance.

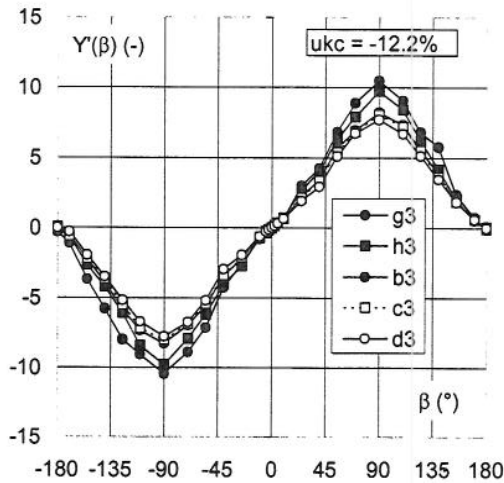


Figure 3.3c. Ship model D. Drift induced lateral force: influence of bottom characteristics for negative under keel clearance.

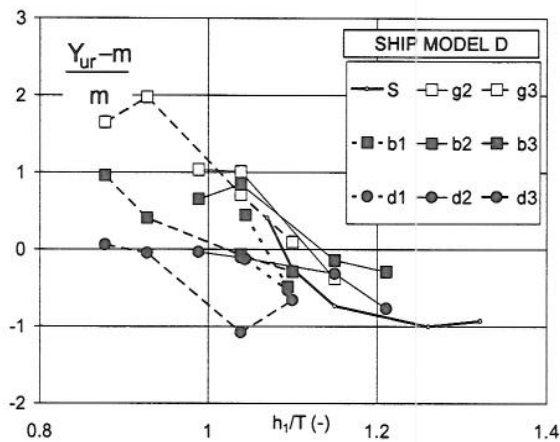


Figure 3.4: Ship model D. Linear yaw velocity derivative for lateral force: influence of bottom characteristics and under keel clearance.

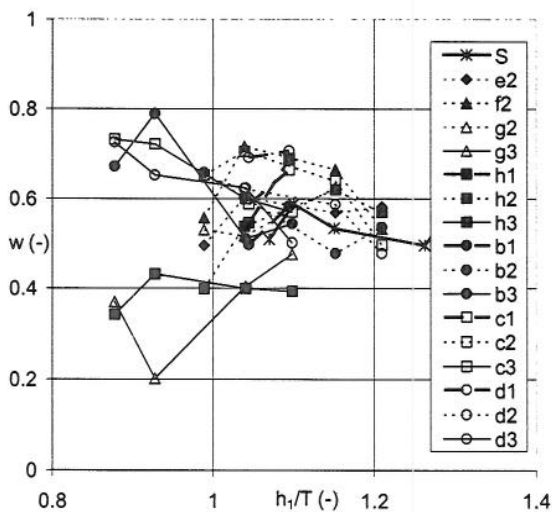


Figure 3.5. Ship model D. Wake factor: influence of bottom characteristics and under keel clearance.

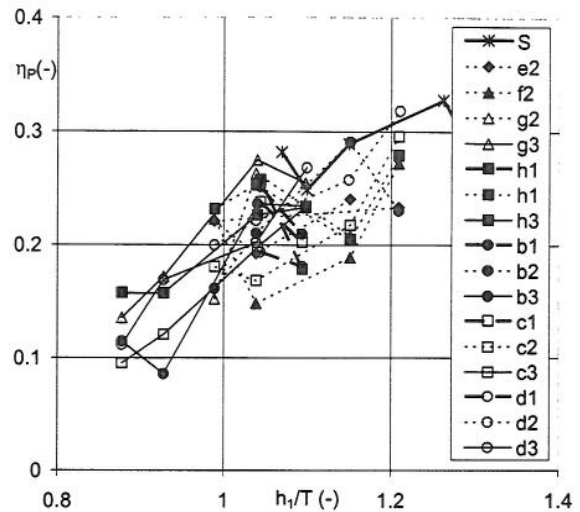


Figure 3.6. Ship model D. Overall propeller efficiency: influence of bottom characteristics and under keel clearance.

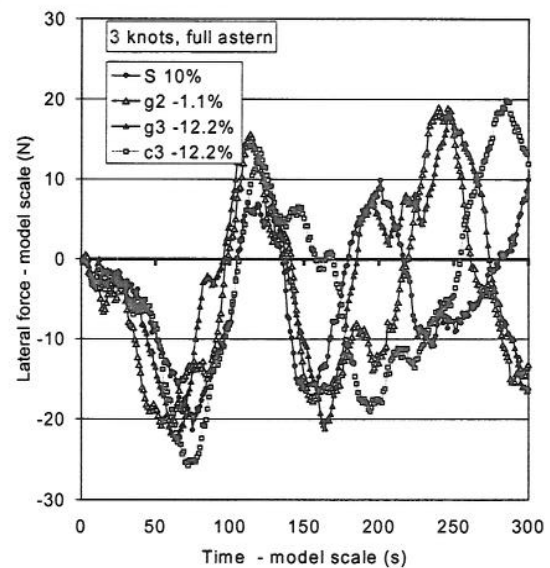


Figure 3.7. Ship model D. Fluctuations of the lateral force due to combinations of forward speed and propeller action astern.

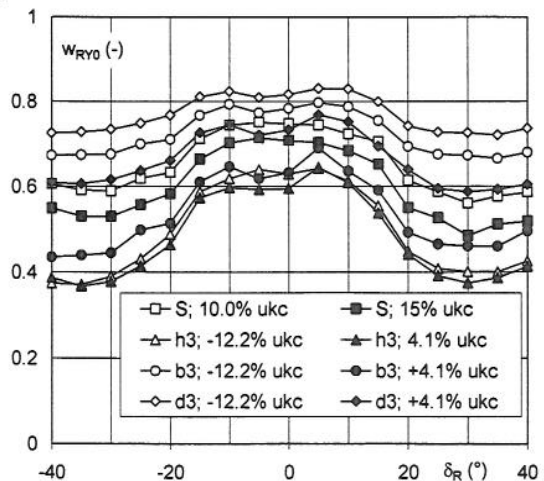


Figure 3.8. Ship model D. Rudder wake factor for lateral rudder force: influence of rudder angle for several combinations of bottom characteristics and under keel clearance.

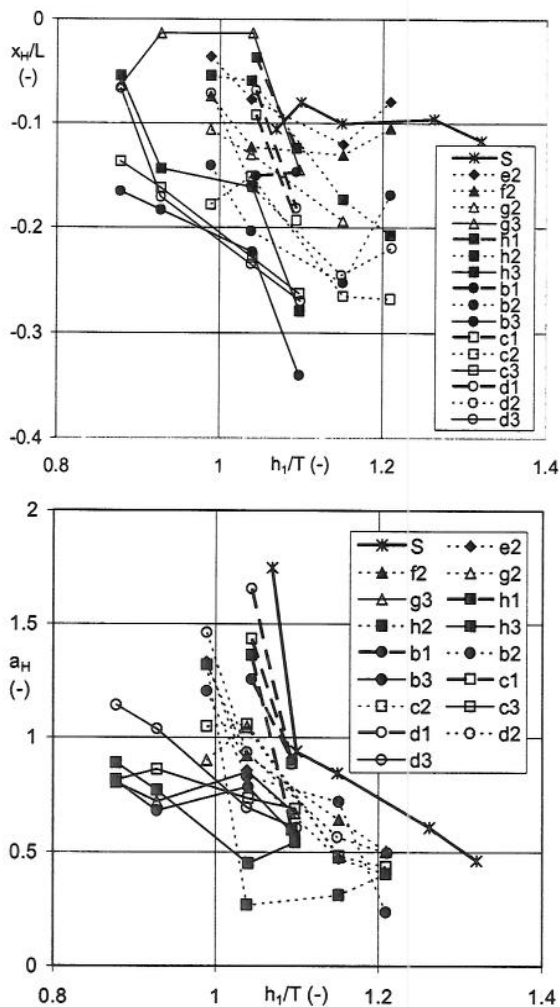


Figure 3.9. Ship model D. Rudder-hull interaction factor a_H and application point position x_H : influence of bottom characteristics and under keel clearance.

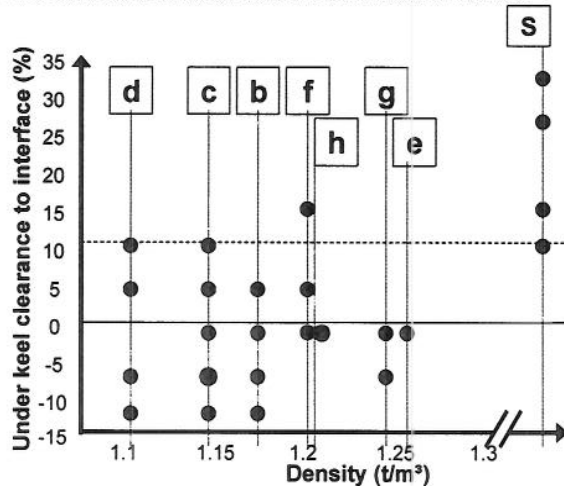


Figure 4.2. Real time simulation program: overview of simulated conditions.

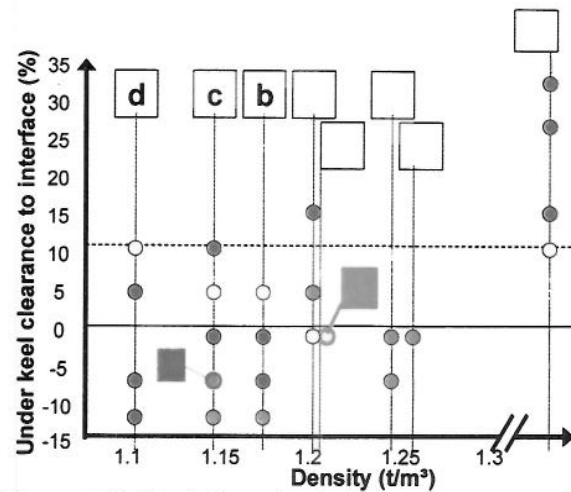


Figure 4.3. Real time simulation program: overall pilots' assessment (1: with extra tug assistance; 2: wind E, 6 Bf)

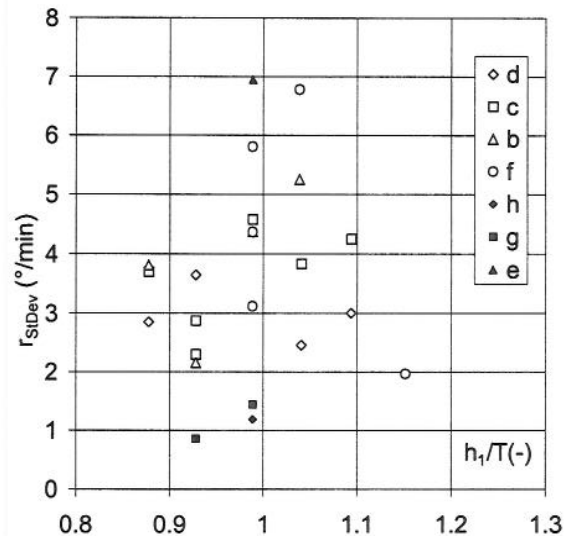


Figure 4.4. Real time simulation program, trajectory 3, sub-trajectory 4. Standard deviation of rate of turn: influence of bottom characteristics and under keel clearance.

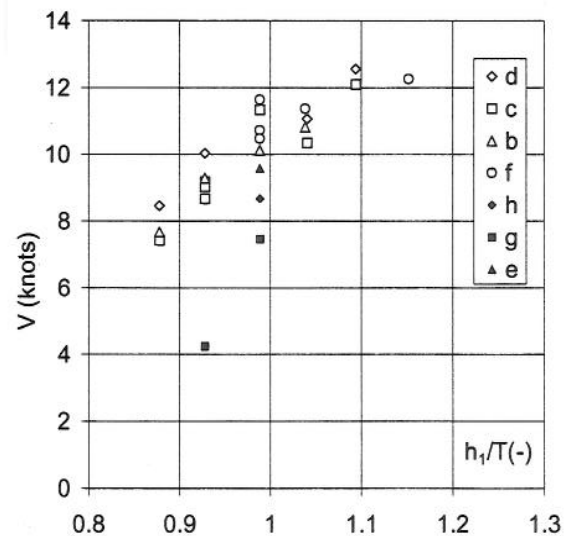


Figure 4.5. Real time simulation program, trajectory 3, sub-trajectory 4. Developed speed: influence of bottom characteristics and under keel clearance.

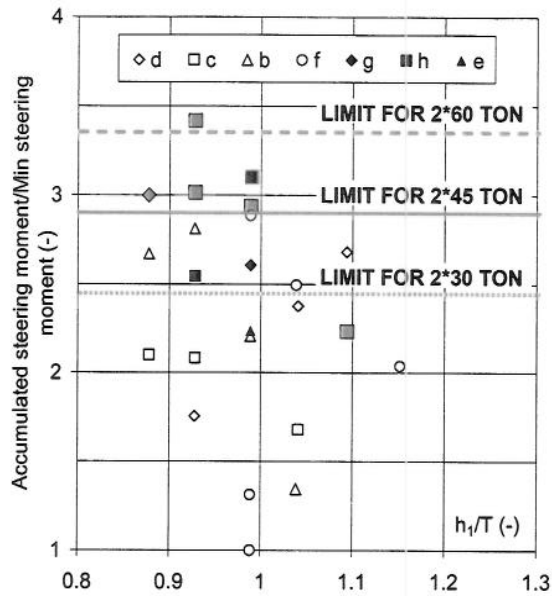


Figure 4.6. Real time simulation program. Steering moment impulse and limits for several tug configurations: influence of bottom characteristics and under keel clearance.

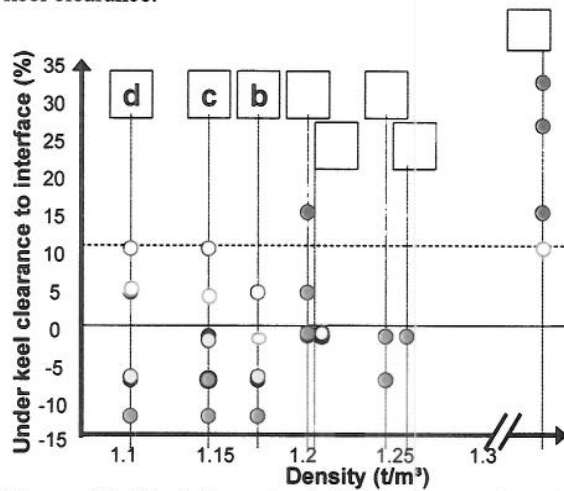


Figure 4.7. Real time simulation program. Acceptability of manoeuvres taking account of all criteria, with assistance of 2 tugs with 45 ton bollard pull each.

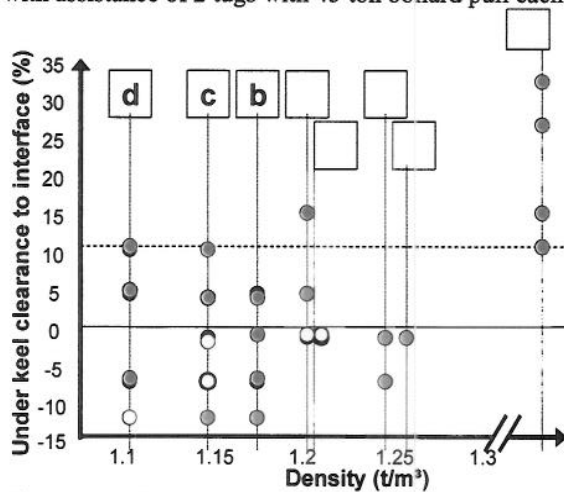


Figure 4.8. Real time simulation program. Acceptability of manoeuvres taking account of all criteria, with assistance of 2 tugs with 60 ton bollard pull each.



Figure 4.1. Real time simulation program: trajectories and sub-trajectories.